

Dielectric relaxation processes in $\text{Cd}_2\text{Nb}_2\text{O}_7$ compound

Chen Ang,^{a)} Ruyan Guo, A. S. Bhalla, and L. E. Cross

Materials Research Laboratory, The Pennsylvania State University, University Park, Pennsylvania 16802

(Received 11 October 1999; accepted for publication 9 February 2000)

This article reports a study on the dielectric relaxation processes of $\text{Cd}_2\text{Nb}_2\text{O}_7$ compound. Three dielectric relaxation modes I, II, and III were reexamined. By using the Cole–Cole equation fitting of the frequency dependence of dielectric constant and loss, we obtained more precise relaxation time data, compared to the data reported in the literature. The results indicate that the relaxation time for mode I follows the Arrhenius law with one slope rather than two slopes as reported in the literature in the frequency range of 10^2 – 10^5 Hz. However, the parameters obtained from the Arrhenius law fit are not physically reasonable. More physically reasonable parameters can be obtained by fitting the relaxation time to the empirical Vogel [Z. Phys. **22**, 645 (1921)]–Fulcher [J. Am. Ceram. Soc. **8**, 339 (1925)] relation with essentially the same fitting quality. A comparison of $\text{Cd}_2\text{Nb}_2\text{O}_7$ with well known triglycine sulphate (TGS) is made. The similarity between the dielectric response of $\text{Cd}_2\text{Nb}_2\text{O}_7$ and TGS is emphasized. The physical mechanism of the relaxation modes is briefly discussed. With increasing dc bias, the three relaxation modes were suppressed and eventually eliminated. This indicates that the dielectric responses of $\text{Cd}_2\text{Nb}_2\text{O}_7$ at zero dc bias are the sum effect of several dielectric modes with relaxation polarization superimposed on the ferroelectric–paraelectric phase transition. © 2000 American Institute of Physics. [S0021-8979(00)03710-5]

I. INTRODUCTION

Ferroelectricity in pyrochlore structure $\text{Cd}_2\text{Nb}_2\text{O}_7$ (CNO) compound was discovered and studied in the 1950's.^{1–4} Two main dielectric anomalies around 85 and 185 K were reported at first as indicated by the measurement of the dielectric behavior. Later, the ferroelectric behavior was extensively studied by Isupov *et al.*,^{5–9} Smolenskii *et al.*,^{10–16} and Kolpakova *et al.*,^{17–26} who reported that there could be up to possibly eight phase transitions as detected by the dielectric, light scattering, electrooptic, and specific heat measurements in CNO. Main attention was focused on what Isupov *et al.*⁸ Smolenskii *et al.*¹² regarded as the “unusual properties”, i.e., in a narrow temperature range of 170–205 K, there are three dielectric anomalies, at ~170–196 K, 196–201 K, and 201–205 K, and also an unusual high-field dependence of the dielectric constant. According to the earlier studies by Smolenskii's^{10–16} and Isupov's^{5–9} groups, the lower temperature dielectric anomaly at ~85 K was attributed to an incommensurate–commensurate phase transition, while three anomalies at ~201–205 K, 196–201 K, and 170–196 K, were attributed to an improper ferroelectric transition, a ferroelectric–ferroelectric transition, and a diffuse ferroelectric phase transition, respectively.

The so-called diffuse ferroelectric transition around 170–196 K is characterized by Swartz *et al.*²⁷ and Kolpakova *et al.*^{22–26} They discussed the temperature dependence of the relaxation time that obtained from the temperature dependence of the imaginary part of the permittivity, and fitted to the Arrhenius law. They found that the relaxation

time versus the inverse temperature ($1/T$) have two different slopes, one in the frequency range of 10 kHz–1 MHz and the other below 10 kHz, respectively. However, the relaxation data for these works have used only a few frequency points (for example, four or five points), so that it is difficult to give a precise description of the physical mechanism. In addition, as we know that in the case of CNO, there are several permittivity peaks within a narrow temperature range, thus it is very difficult to obtain the precise relaxation times from the temperature dependence of the imaginary part of the overlapped permittivity peaks.

In this article, we have reexamined the dielectric relaxation process and obtained the more precise relaxation times from the Cole–Cole equation fitting of the frequency dependence of the dielectric constant and loss. This method was also adopted to analyze the other two relaxation processes observed below the diffuse ferroelectric transition around 185 K. The relaxation time versus the inverse temperature thus obtained follows the Arrhenius law in the frequency range of 10^2 – 10^5 Hz. In addition, with the application of a dc bias, the CNO system shows that the relaxation processes can be suppressed and eliminated. This phenomenon suggested that the dielectric response at zero field could be recognized as the relaxation processes superimposed on the paraelectric–ferroelectric phase transition behavior.

II. EXPERIMENTAL PROCEDURES

The ceramic samples of CNO were prepared by the solid state reaction. The samples are of single phase. The detailed process for the samples preparation is described in Ref. 27. Complex dielectric permittivity was measured using a Hewlett Packard 4284 LCR bridge with the ac field of 1

^{a)}On leave from Department of Physics, Zhejiang University, Hangzhou, 310027, People's Republic of China; electronic mail: angchen@psu.edu

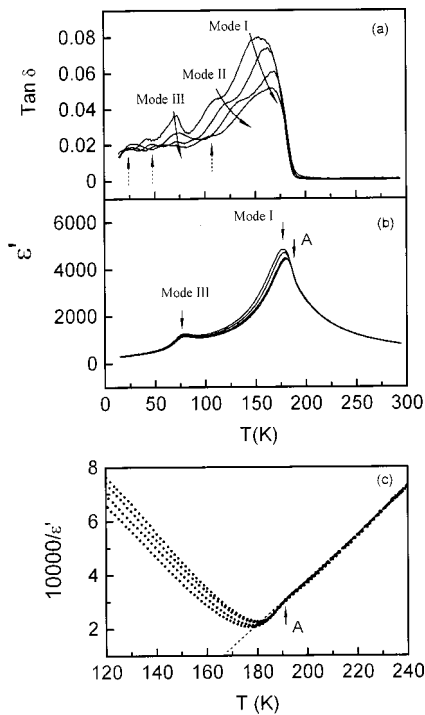


FIG. 1. Temperature (T) dependence of $\tan \delta$ (a), ϵ' (b), and $1/\epsilon'$ (c) for the $\text{Cd}_2\text{Nb}_2\text{O}_7$, at 0.1, 1, 10, and 100 kHz, from top to bottom for (a) and (b), from bottom to top for (c). The dash line in (c): Fits to Curie–Weiss law.

V/mm. The temperature dependence of the dielectric properties was measured in a cryostat system in the temperature range 10–300 K, while the specimen was being cooled or heated up at a typical cooling/heating rate of 1 K per minute and readings were taken at 1 or 2 K intervals. A dc voltage was applied to the samples and a blocking circuit was adopted to separate the high dc voltage from the LCR meter.

III. RESULTS AND DISCUSSION

A. Dielectric properties in CNO ceramic

The temperature (T) dependence of the dielectric constant (ϵ'), the dissipation factor ($\tan \delta$), and the reciprocal dielectric constant ($1/\epsilon'$) for CNO are shown in Figs. 1(a)–1(c). It can be seen that:

(1) From the $\tan \delta$ versus T curve, as shown in Fig. 1(a), at first glance, there are three obvious relaxation modes, denoted as modes I, II, and III, whose temperature of the peak maxima (T_m) shifts to a higher temperature with increasing frequency. By careful inspection, a small peak can be noticed (marked by a dashed arrow) at a temperature slightly higher than that of mode III. Below mode III, there are two more peaks, also marked by the dashed arrows. These small anomalies were also reported by Isupov *et al.*⁹ and Smolenskii *et al.*¹⁰

(2) In the ϵ' versus T curve, we observe two main peaks at ~ 178 and 80 K (at 1 kHz), which correspond to mode I and mode III, respectively. However, for Mode II, ϵ' only shows a frequency dispersion without any peak. For the other small anomalies observed in the $\tan \delta$ versus T , there are no corresponding anomalies occurring for the ϵ' versus

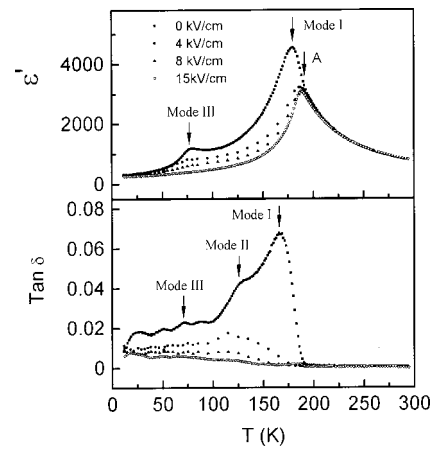


FIG. 2. Temperature dependence of ϵ' of the $\text{Cd}_2\text{Nb}_2\text{O}_7$ at 5 kHz under dc fields.

T . This indicates that for ϵ' versus T , the corresponding peaks (including mode II) are overlapped by the mode I and mode III, which have higher magnitudes.

(3) For anomalies in the higher temperature region (170–200 K), Isupov and Tarasova⁹ and Smolenskii *et al.*¹² reported that there are three dielectric anomalies. In the present work, we have observed mode I at ~ 178 K, and a clear anomaly at 192 K in the temperature dependence of the $1/\epsilon'$, which is denoted as peak A. We did not find a dielectric anomaly around 200 K, which was reported by Smolenskii *et al.*¹² However, a slight indication of such an anomaly was noticed if the data fitted to the Curie–Weiss law (not shown here).

(4) Comparing the earlier results reported in the literature with the present results, the various modes can be classified as follows: (a) Mode I at ~ 178 K, is so-called ‘‘diffuse phase transition’’,^{9,11,24,25} (b) Mode III is the dielectric anomaly that is attributed to an incommensurate phase transition.^{9,20} (c) Mode II is observed in some earlier work.¹¹ (d) Peak A is a ferroelectric–paraelectric phase transition.^{9,12}

It should be emphasized that these relaxation processes have been observed in both single crystals and ceramics,^{9,11,22–27} and therefore are not pertinent to grain boundary effects.

In this article, we will further discuss the dielectric relaxation anomalies, mode I, mode II, and mode III. Peak A and the small peaks marked by the dashed arrows in the Fig. 1(a) will be discussed elsewhere.

B. Temperature dependence of dielectric property under dc fields

The temperature dependence of the dielectric constant and $\tan \delta$ under dc fields at 5 kHz is shown in Fig. 2. It can be seen that the dielectric modes I, II, and III are suppressed obviously by the application of the dc electric fields, and then Peak A becomes visible. At the dc field of 15 kV/cm, mode I, modes II and III almost disappear. With further increasing dc fields, unlike all known ferroelectrics, the permittivity maximum of the Peak A remains almost the same, while T_C shifts to lower temperatures. The detailed discussion on Peak A will be given elsewhere.²⁸

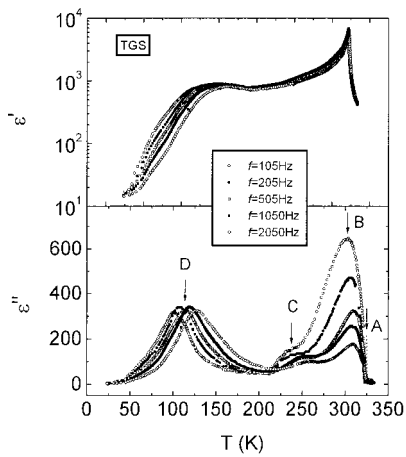


FIG. 3. Temperature dependence of the real and imaginary parts of the permittivity (ϵ' and ϵ'') as a function of frequency for TGS. The data are from Professor Wang.

Based on this observation, we suggest that the dielectric behavior of CNO without dc bias is the sum effect of modes I, II, and III (also including the small modes which are observed in $\tan \delta$ versus T at zero field) with Peak A. From this point of view, the dielectric behavior of CNO is similar to that of Bi doped SrTiO_3 solid solutions, which display sum effect of several dielectric defect modes and a ferroelectric relaxor mode superimposed on a background of quantum paraelectric behavior.^{29,30}

C. Comparison with other systems

For many ferroelectric compounds and solid solutions, like TGS, potassium dihydrogen phosphate (KDP), etc., it is observed that in the lower temperature side of Curie temperature, T_c , the dielectric constant exhibits an unusually high value as compared to that as predicated by the phenomenological Landau theory, and also shows a plateau-like temperature dependence.^{31–36} Subsequently, at a temperature T_f , the dielectric constant abruptly drops to its phenomenological value. The large difference of ϵ' between $T_f < T < T_c$, is believed to be due to the motion of domain walls. Wang's group^{37,38} reported that, for TGS, as shown in Fig. 3, the ϵ' shows a sharp peak at a higher temperature 320 K, and a diffused, rounded peak at a lower temperature ~ 125 K. However, the ϵ'' shows three peaks around higher temperature transition, that is, a sharp peak with very narrow width of peak at 320 K (A), another peak a few degrees Kelvin lower at ~ 310 K (B), and the diffused peak around 235 K (C). Corresponding to the diffused ϵ' peak around ~ 125 K, the ϵ'' shows also a diffused rounded peak.^{37,38}

Comparing Fig. 1 with Fig. 3, we found an obvious similarity between the behavior of TGS and CNO. Also, below the T_c , there is no additional genuine ferroelectric phase transition occurs down to 10 K regardless of the existence of the dielectric anomalies in this temperature range.

D. Dielectric relaxation behavior

In order to gather more information concerning the polarization processes associates with modes I, II, and III,

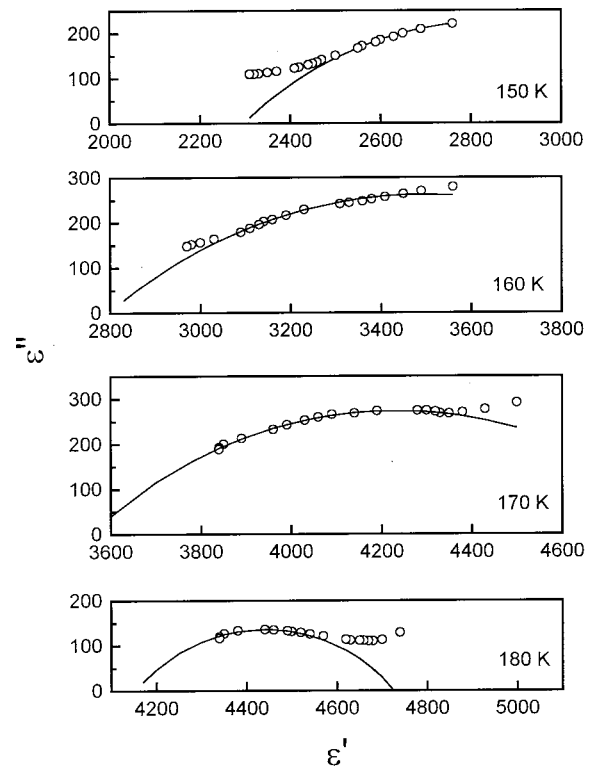


FIG. 4. Cole–Cole plot (ϵ' vs ϵ'') of the $\text{Cd}_2\text{Nb}_2\text{O}_7$ at 150, 160, 170, and 180 K [open circles: Experimental data; Circular arcs: Fits to the experimental data by using Eq. (1)].

Cole–Cole equation was adopted to better obtain the relaxation times of these modes. Figure 4 shows the Cole–Cole plot for mode I. As shown in Fig. 4, the data points fit into a semicircular arc with the center lying underneath the abscissa. The complex permittivity can be empirically described by the Cole–Cole equation:³⁹

$$\epsilon^* = \epsilon_\infty + (\epsilon_0 - \epsilon_\infty) / [1 + (i\omega\tau)^\beta], \quad (1)$$

where ϵ_0 is the static permittivity, ϵ_∞ is the permittivity at high frequency, ω is the angular frequency, τ is the mean relaxation time, and $\beta = 1 - \alpha$, where α is the angle of the semicircular arc. By fitting this arc with the least square approach, for mode I, $\epsilon_0 = 4869$, $\epsilon_\infty = 3937$, and $\beta = 0.484$ at 176.5 K, were obtained. In the temperature interval 150–190 K, β is in the range of 0.44–0.6.

The real and imaginary parts of the permittivity can be rewritten from Eq. (1) in the following way:

$$\epsilon' = \epsilon_\infty + (\Delta\epsilon'/2) \{1 - \sinh(\beta z) / [\cosh(\beta z) + \cos(\beta\pi/2)]\}, \quad (2)$$

$$\epsilon'' = (\Delta\epsilon'/2) \sin(\beta\pi/2) / [\cosh(\beta z) + \cos(\beta\pi/2)], \quad (3)$$

where $z = \ln(\omega\tau)$ and $\Delta\epsilon' = \epsilon_0 - \epsilon_\infty$. Frequency dependence of ϵ' and ϵ'' for mode I, II, and III at several temperatures and the corresponding fitting curves are shown in Fig. 5.

If the dielectric relaxation is related to a thermally activated process, the relaxation time will obey the Arrhenius law

$$\tau = \tau_0 \exp[U/(k_B T)], \quad (4)$$

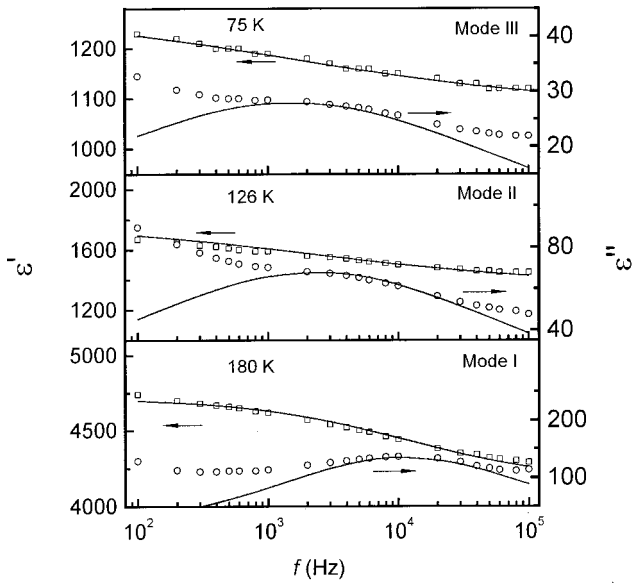


FIG. 5. Frequency dependence of ϵ' and ϵ'' for mode I, II, and III at some temperatures. Open squares and circles: Experimental data; Solid curves: Fits to the experimental data by using Eqs. (1)–(3).

where τ_0 is the relaxation time at infinite temperature, U the activation energy for relaxation, k_B the Boltzmann's constant, and T the absolute temperature.

Using Eqs. (2) and (3), the relaxation time was calculated for mode I from 150 to 190 K, for mode II from 106 to 146 K, and for mode III from 70 to 95 K. The relaxation rate ν ($\nu=1/2\pi\tau$) plotted against the reciprocal of the absolute temperature ($1/T$) is shown in Fig. 6. The relation between $\log \nu$ and $1/T$ is linear and this linear relation gave an activation energy for the relaxation process, $U=0.38$ eV, $\tau_0=1.8\times 10^{-16}$ s for mode I. The same procedures were carried out for modes II and III, the corresponding parameters for mode I, II, and II are summarized in Table I.

From Table I, it can be seen that the parameters for mode I, $\tau_0=1.8\times 10^{-16}$ s (corresponding to a frequency 1.7×10^{15} Hz), seem to be too high for the system. Due to this reason, and as discussed in Sec. II, we have tried to fit the Vogel–Fulcher relation⁴⁰ for mode I

$$\tau = \tau_0 \exp\left\{E/[k_B \cdot (T - T_{VF})]\right\}, \quad (5)$$

where τ is the relaxation time, τ_0 is the pre-exponential term, E is the hindering barrier, T_{VF} is the Vogel–Fulcher temperature and k_B is the Boltzmann constant. Almost the same fit-

TABLE I. The activation energy, preexponential term, and Vogel–Fulcher temperature of the Arrhenius law and the Vogel–Fulcher relation for the modes I, II, and III in $\text{Cd}_2\text{Nb}_2\text{O}_7$ compound.

		Mode I	Mode II	Mode III
Arrhenius law	τ_0 (s)	1.8×10^{-16}	2×10^{-15}	2×10^{-14}
	U (eV)	0.39	0.26	0.16
Vogel–Fulcher relation	τ_0 (s)	0.9×10^{-12}	0.62×10^{-12}	0.62×10^{-12}
	E (eV)	0.21	0.19	0.14
	T_{VF} (K)	45	18.5	5

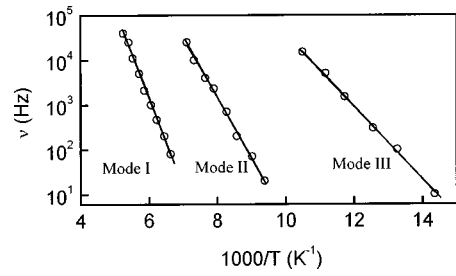


FIG. 6. Relaxation rate ν ($\nu=1/2\pi\tau$) vs $1/T$ curve. Open circles: Experimental data; Lines: Fitting to the Arrhenius law, Eq. (4) and the Vogel–Fulcher relation, Eq. (5). Because the fitting quality for the Arrhenius law and the Vogel–Fulcher relation is almost the same, the lines are overlapped.

ting quality is obtained for the empirical Vogel–Fulcher relation, as shown in Fig. 6. However, comparing with the Arrhenius law, for the empirical Vogel–Fulcher, the physically reasonable parameters $T_{VF}=45$ K, $E=0.21$ eV, $\tau_0=0.9\times 10^{-12}$ s were obtained. For comparison, we also fitted the modes II and III to Vogel–Fulcher relation, as shown in Fig. 6 and the fitting parameters are listed in Table I, respectively.

The relaxation time of modes II and III obtained in the frequency range 10^2 – 10^5 Hz could be fitted to both the Arrhenius law and the Vogel–Fulcher relation with the reasonable physical parameters. Lyons, Fleury, and Rytz⁴¹ reported that, for $\text{KTa}_{0.991}\text{Nb}_{0.009}\text{O}_3$, only considering the relaxation time obtained in the low frequency range, the relaxation time follows well the Arrhenius law (it also can be fitted well to Vogel–Fulcher relation); however, after extending the frequency to a higher range, up to $\sim 10^{10}$ Hz, the relaxation time follows the Vogel–Fulcher relation rather than the Arrhenius law. For the CNO system, it will be interesting to test the validation of the Arrhenius law and the Vogel–Fulcher relation after extending the measurements to higher frequencies.

E. Discussion

Based on the comparison of CNO with TGS in Sec. III B, i.e., the dielectric anomalies in CNO are very similar to those observed in TGS, where a model of freezing of domain walls below T_c is widely accepted. In the case of CNO, Kolpakova *et al.*¹⁷ and Smolenskii *et al.*¹⁵ reported that ferroelectric and/or ferroelastic domains appear around ~ 200 K, and change the domain structure at ~ 200 , ~ 190 , and ~ 180 K. This indicates the complexity of the domain structure and probably also of the motion of domain walls in CNO. Based on the similarity between CNO and TGS, and the fact that more suitable physical parameters can be obtained by fitting the relaxation times to the Vogel–Fulcher relation, it is reasonable to assume that mode I is due to the motion of the domain walls below the paraelectric–ferroelectric phase transition around 190 K. Mode II might also be attributed to the motion of the domain walls similar to the mode I and the peaks in TGS/KDP.^{37,38}

However, on the other hand, Kolpakova *et al.*²⁴ also pointed out that $\text{Cd}_2\text{Nb}_2\text{O}_7$ belongs to the cubic oxide pyrochlores of $\text{Cd}_2\text{Nb}_2\text{O}_6\text{Z}$ type (Z denotes the “seven oxygen”

ions O, S, OH, or F). Because of the special structural characteristics of CNO, the “seventh” oxygen ions are weakly bonded to the $(\text{NbO}_6)^n$ octahedral, which form the structural framework of the lattice. The reorientation of the seventh oxygen with Cd dipoles²⁴ under ac external electric fields, will cause the dielectric relaxation. This is similar to the “defect modes” observed in Bi doped SrTiO_3 .^{29,30} At this stage, we can not give a definite conclusion, and further work is being conducted.

Mode III at ~ 85 K was attributed to an incommensurate–commensurate phase transition in earlier literature.^{9,16–18} In the present work, we have observed that this mode displays a relaxation behavior and it can be suppressed and finally eliminated by the application of dc bias of ~ 15 kV/cm. A clear understanding of the physical nature of mode III also requires more experimental data.

IV. CONCLUSION

In this article, we have reexamined the dielectric relaxation processes in CNO. The more precise relaxation times were obtained from the Cole–Cole equation fitting of the frequency dependence of dielectric constant and loss. For mode I, the so-called “diffuse ferroelectric transition” around 185 K, the relaxation time versus the inverse temperature in the frequency range 10^2 – 10^5 Hz follows well the Arrhenius law but with unreasonable physical parameters. However, the data could be fitted well to the empirical Vogel–Fulcher relation with much more reasonable physical parameters. For modes II and III, the relaxation time follows well both the Arrhenius law and the empirical Vogel–Fulcher relation with reasonable physical parameters.

A comparison with well known dielectric behavior of TGS is made. Similar to the dielectric properties of TGS, mode I could be attributed to the motion of domain walls and the possible freezing in CNO. Mode II might be due to the motion of domain walls or defect modes. However, the contribution from the possible reorientation of the seventh oxygen with Cd dipoles in the special crystalline structure of CNO under ac external fields could be an alternative explanation. A clear understanding of the physical mechanism for these dielectric modes needs further work.

We observed that modes I, II, and III with dielectric relaxation behavior can be suppressed and finally eliminated under high dc fields. This indicates that the dielectric response of CNO is the sum effect of modes I, II, and III superimposed on the background of the ferroelectric–paraelectric phase transition peak A.

ACKNOWLEDGMENTS

The authors thank, particularly, Professor Y. N. Wang (Nanjing University, China) for providing us with Fig. 3. One of the authors (C. A.) would like to thank Dr. Zhi Yu for the stimulating discussion. This work was supported by a grant from DARPA under Contract No. DABT63-98-1-002.

- ²G. Shirane and R. Pepinsky, *Phys. Rev.* **92**, 504 (1953); J. K. Hulm, *ibid.* **92**, 504 (1953).
- ³F. Jona, *Phys. Rev.* **98**, 903 (1955); H. Danner and R. Pepinsky, *ibid.* **99**, 1215 (1955).
- ⁴A. deBretteville *et al.*, *J. Am. Ceram. Soc.* **48**, 86 (1957).
- ⁵V. A. Isupov and O. K. Khomutetskii, *J. Tech. Phys. (USSR)* **27**, 2513 (1957).
- ⁶V. A. Isupov and V. N. Skubitskii, *Sov. Phys. Solid State* **5**, 957 (1963).
- ⁷G. I. Golovshchikova, V. A. Isupov, and I. E. Myl'nikova, *Sov. Phys. Solid State* **13**, 2349 (1971).
- ⁸V. A. Isupov, G. I. Golovshchikova, and I. E. Myl'nikova, *Ferroelectrics* **8**, 507 (1974).
- ⁹V. A. Isupov and G. I. Tarasova, *Sov. Phys. Solid State* **25**, 584 (1983); **25**, 587 (1983).
- ¹⁰G. A. Smolenskii, N. N. Kolpakova, S. A. Kizhaev, and I. G. Siny, *Ferroelectr. Lett. Sect.* **44**, 129 (1982).
- ¹¹G. A. Smolenskii, N. N. Krainik, L. S. Kamzina, F. M. Salaev, S. N. Dorogovtzev, and E. S. Sher, *Ferroelectrics* **55**, 321 (1984).
- ¹²G. A. Smolenskii, N. N. Krainik, L. S. Kamzina, F. M. Salaev, E. A. Tarakanov, and E. S. Sher, *Jpn. J. Appl. Phys., Suppl.* **24-2**, 820 (1985).
- ¹³F. M. Salaev, L. S. Kamzina, N. N. Krainik, G. A. Smolenskii, and N. A. Morozov, *Sov. Phys. Solid State* **26**, 1808 (1984).
- ¹⁴L. S. Kamzina, F. M. Salaev, N. N. Krainik, S. N. Dorogovtzev, and G. A. Smolenskii, *Sov. Phys. Solid State* **25**, 1645 (1983).
- ¹⁵F. M. Salaev, L. S. Kamzina, N. N. Krainik, E. S. Sher, and G. A. Smolenskii, *Sov. Phys. Solid State* **25**, 89 (1983).
- ¹⁶G. A. Smolenskii, N. N. Kolpakova, S. A. Kizhaev, and E. S. Sher, *Ferroelectrics* **73**, 161 (1987).
- ¹⁷N. N. Kolpakova, I. G. Sini, M. Polomska, and R. Margraf, *Sov. Phys. Solid State* **24**, 985 (1982).
- ¹⁸N. N. Kolpakova, R. Margraf, A. Pawlowski, A. Pietraszko, L. Szczepanska, I. S. Barash, and E. S. Sher, *Sov. Phys. Solid State* **29**, 2078 (1987).
- ¹⁹N. N. Kolpakova, M. Polomska, R. Margraf, and E. S. Sher, *Ferroelectrics* **106**, 93 (1990).
- ²⁰N. N. Kolpakova, B. Hilczler, and M. Wiesner, *Phase Transit.* **47**, 113 (1994).
- ²¹N. N. Kolpakova, M. S. Waplak, and W. Bednarski, *J. Phys.: Condens. Matter* **10**, 9309 (1998).
- ²²N. N. Kolpakova, M. Wiesner, I. L. Shul'pina, and P. Piskunowicz, *Ferroelectrics* **190**, 91 (1999).
- ²³N. N. Kolpakova, M. Polomska, and J. Wolk, *Ferroelectrics* **126**, 151 (1992); N. N. Kolpakova, M. Polomska, and R. Margraf, *Sov. Phys. Solid State* **32**, 1106 (1990).
- ²⁴N. N. Kolpakova, M. Wiesner, G. Kugel, P. Bourson, *J. Phys.: Condens. Matter* **6**, 2787 (1994).
- ²⁵N. N. Kolpakova, M. Wiesner, G. Kugel, P. Bourson, *Ferroelectrics* **190**, 179 (1997).
- ²⁶N. N. Kolpakova, M. Wiesner, A. O. Lebedev, P. P. Syrnikov, and V. A. Khramstov, *Tech. Phys. Lett.* **24**, 679 (1998).
- ²⁷S. L. Swartz, C. A. Randall, and A. S. Bhalla, *J. Am. Ceram. Soc.* **72**, 637 (1989).
- ²⁸C. Ang, R. Guo, A. S. Bhalla, and L. E. Cross (unpublished).
- ²⁹C. Ang, J. F. Scott, Z. Yu, H. Ledbetter, and J. L. Baptista, *Phys. Rev. B* **59**, 6661 (1999).
- ³⁰C. Ang, Z. Yu, J. Hemberger, P. Lunkenheimer, and A. Loidl, *Phys. Rev. B* **59**, 6665 (1999); **59**, 6670 (1999).
- ³¹K. L. Bye, P. W. Whipps, and E. T. Keve, *Ferroelectrics* **4**, 253 (1972).
- ³²E. Nakamura, K. Kuramoto, K. Deguchi, and K. Hayashi, *Ferroelectrics* **98**, 363 (1989).
- ³³E. Nakamura, *Ferroelectrics* **135**, 237 (1992).
- ³⁴E. Nakamura, K. Deguchi, K. Kuramoto, I. Hirata, T. Ozaki, and J. Ogami, *Ferroelectrics* **140**, 157 (1993).
- ³⁵J. Bornarel and B. Torche, *Ferroelectrics* **132**, 273 (1992).
- ³⁶L. N. Kamysheva and S. N. Drozhdin, *Ferroelectrics* **71**, 281 (1987).
- ³⁷Y. N. Huang, Y. N. Wang, and H. M. Shen, *Phys. Rev. B* **46**, 3290 (1992).
- ³⁸Y. N. Huang, X. Li, Y. Ding, Y. N. Wang, H. M. Shen, Z. F. Zhang, C. S. Fang, and P. C. W. Fung, *Phys. Rev. B* **55**, 16 159 (1997).
- ³⁹K. S. Cole and R. H. Cole, *J. Phys. Chem.* **9**, 341 (1941).
- ⁴⁰H. Vogel, *Z. Phys.* **22**, 645 (1921); G. Fulcher, *J. Am. Ceram. Soc.* **8**, 339 (1925).
- ⁴¹K. B. Lyons, P. A. Fleury, and D. Rytz, *Phys. Rev. Lett.* **57**, 2207 (1986).

¹E. Wainer and Ch. Wentworth, *J. Am. Ceram. Soc.* **55**, 207 (1952); W. R. Cook and H. Jaffe, *Phys. Rev.* **88**, 1426 (1952); **89**, 1297 (1953).